SLAC RADIATION PHYSICS NOTE RP-98-1

TITLE: Response of BCS Ion Chambers Near Stoppers: Simulation and Measurement

AUTHORS: W. R. Nelson, A. Fasso, W. R. Kroutil and G. Nelson

DATE: 16 January 1998

SUMMARY

In this paper we demonstrate experimentally that we can use the EGS4 code to calculate the average current measured by air-filled ion-chambers placed near stoppers that are struck by high-energy electron beams. This paper also shows that it is possible to find a position along the direction of the beam where the radiation pattern is approximately the same for various combinations of a two-stopper system, provided that they are reasonably close to one another.

1. Introduction

Ionization chambers (ICs) have been used as a means of limiting beam power to machine devices (*e.g.*, stoppers, collimators, *etc.*) since the beginning of SLAC and they continue to be an integral part of both the Machine Protection System (MPS) and the Beam Containment System (BCS). When used with the BCS, a pair of ICs is generally placed symmetrically about each device of concern in order to provide some level of redundancy for shutting off the beam before damage occurs.

In recent years, the Radiation Safety Committee has approved the use of a single pair of BCS ICs for the special case where two stoppers are relatively close to one another, provided that it can be demonstrated that they will shutoff the beam under all stopper-in configurations. At SLAC there are three locations where we are currently using a single pair of ICs; namely, the PEP-II Extraction-Line stoppers at Sectors 4 and 10, and the BAS-II Mode stoppers near the end of Sector 28. The best location for these IC pairs was predetermined by means of EGS4[1] Monte Carlo calculations. The trip levels were then established experimentally by actually running electron beams into each stopper.

In this paper we analyze the results of the calibration measurements that were made at Sector 10 on September 25, 1997 for IC-4047 and IC-4048.

2. Monte Carlo Simulations

The two stoppers at Sector 10 are rectangular in shape—*i.e.*, they are 8-inch long Cu blocks having a 3.5×4 sq.inch surface for electron beams to strike. They are separated from one another by a distance of 21-inches (center to center) and they are located inside cylindrical, stainless steel vacuum cans with 1/8-inch thick walls. For our EGS4 calculations we have chosen a cylinder-slab geometry in order to gain statistical advantage from the symmetry. The geometry is shown at the top of Figure 1, where the vacuum cans and the air-filled ICs are depicted as circles, but were actually not part of the simulation. Furthermore, Z boundaries were assigned every 4-cm, but not all of them are shown in Figure 1a to simplify the picture.

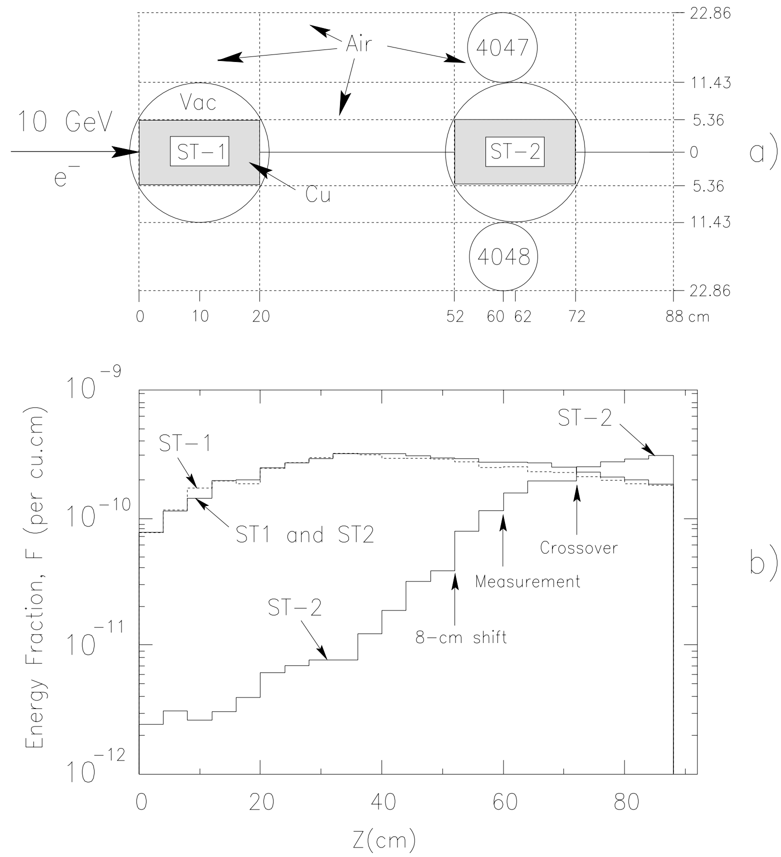

Fig. 1 a) Cylinder-slab geometry, b) Energy deposited in air ($11.43 \leq R < 22.86$ cm).

Three separate calculations were done (30,000 cases each) for the following stopper-in configurations

1. ST-1 Only,
2. ST-2 Only,
3. ST-1 and ST-2.

The fraction of energy deposited (per cm^3) in the outer air cylinder, F, is shown in Figure 1b as a function of Z for each of these stopper configurations. From this plot it appears as if the "crossover" locations of the three histograms is near $Z = 72$ cm.

3. Average Saturation Currents in the Ion Chambers

The rate of ionization in the air cylinder, ρ_0, is obtained from

$$\rho_0 \text{ (esu/cm}^3\text{p)} = \left(\frac{10 \times 10^9 \text{ eV/e}^-}{34 \text{ eV/i.p.}}\right)(4.80 \times 10^{-10} \text{ esu/i.p)} \ I_{beam} \text{ (e}^-\text{/p)} \ F \text{ (cm}^{-3}\text{)} ,$$

where I_{beam} is the beam intensity of the pulse.

The BCS ion chambers (IC-4047 and 4048) at Sector 10 are made up of 32 circular aluminum wafers, 0.0406-cm thick with a radius of 8.89-cm, that are parallel to one another and separated by a gap of 0.615-cm. Small half circles ($r \sim 1.8$ cm) have been cut out at three symmetric locations around the periphery of each to permit alternating wafers to be connected to one another by means of spacers. A potential of 194 V is applied across every other plate in order to form *small sub-chambers* and reduce recombination. The charge from each sub-chamber is summed. The plate structure is isolated within an aluminum cylinder containing air at 1-atm and the total *active volume* (*i.e.*, between the wafers) is 924 cm^3.

The saturation current*, I_0, averaged over many pulses at 10 Hz, is determined from

$$I_0\ (\mu\text{A}) = \rho_0\ (\text{esu/cm}^3\text{p})\ (924\ \text{cm}^3)\ (10\ \text{p/s}) \left(\frac{1.60 \times 10^{-19}\ \text{Coul}}{4.80 \times 10^{-10}\ \text{esu}} \right) \left(\frac{10^6\ \mu\text{A}}{\text{Coul/s}} \right)$$

From these two expressions, it is clear that I_0 should increase linearly with I_{beam}, provided that recombination within the pulse is small.

4. Calibration Measurements

Experimental data was taken with a 10 GeV electron beam at 10 Hz for each of the three stopper-in configurations. The beam intensity, I_{beam}, varied from 0 to 3.5×10^{10} e$^-$/p. The IC-pair was not positioned at the $Z = 72$ cm "crossover" point suggested above, but at a location somewhere between $52 \leq Z \leq 60$ cm (probably closer to the latter). The results are presented in Table 1†.

Table 1. Measurement of the average current $I(\mu\text{A})$ vs. electron beam intensity $I_{beam}(\text{e}^-/\text{p})$ for various stopper configurations, at 10 GeV and 10 Hz (DC offset not subtracted).

I_{beam}	ST-1 Only		ST-2 Only		ST-1 and ST-2	
($\times 10^{10}$ e$^-$/p)	IC-4047	IC 4048	IC-4047	IC-4048	IC-4047	IC-4048
0.0	0.21$^{a)}$	0.19$^{a)}$	0.21$^{a)}$	0.19$^{a)}$	0.21$^{a)}$	0.19$^{a)}$
0.5	0.6061	0.6261	0.3601	0.3134	0.6303	0.6706
1.0	0.9804	0.9760	0.4873	0.4189	0.9648	0.8130
1.5	1.569	1.413	0.6813	0.6012	1.451	1.261
2.0	1.490	1.322	0.7539	0.5995	1.666	1.337
2.5	1.897	1.872	0.9364	0.7516	1.615	1.445
3.0	2.145	1.800	1.084	0.7712	2.119	1.719
3.5	2.308	2.294	1.189	0.7659	2.442	1.991

a) DC offset

∗ Saturation implies full collection of all of the charge of one sign produced between the IC plates.

† We thank the SLAC Accelerator Operators, T. Marsh and M. Saleski, for recording this data.

From the above tabulation, it is apparent that the average current does not increase linearly with beam intensity as expected. The most probable explanation for this is that the rate of ionization is very large and significant recombination is taking place. We will address this issue in the next section.

5. Average Current Corrected for Recombination

A free electron produced in an ionizing event may become attached to a neutral gas atom, thus making a negative ion. This is very likely to happen in an *electronegative* gas, such as air, as opposed to a *non-electronegative* gas, such as argon. In general, it is much easier to collect all of the charge released in an ion chamber filled with argon than one filled with air because the drift velocity of free electrons is about 1000 times larger than that of ions. Thus recombination is much more likely to be a problem in air-filled ICs, such as the ones we are currently using at Sector 10.

A theory has been worked out by Boag[2] for general recombination in pulsed fields. It is applicable to our situation, since each pulse is very short (< 3 nsec) and the time between pulses is large (100 msec) at 10 Hz. The drift velocity of the ions in each sub-chamber is given by

$$v = kV/d \text{ (cm/s)},$$

where

$$\begin{aligned} V &= \text{applied potential} = 194 \text{ V}, \\ d &= \text{chamber gap} = 0.615 \text{ cm}, \\ k &= \text{ion mobility (cm/s)/(V/cm)} \\ &= 1070 \text{ (+ ions)}^{[2]} \\ &= 1350 \text{ (− ions)}^{[2]}, \end{aligned}$$

and the *transit time* for ions to cross the gap calculates to be

$$\begin{aligned} t = d/v = d^2/kV &= 1.8\mu\text{s (+ ions)} \\ &= 1.4\mu\text{s (− ions)}. \end{aligned}$$

Therefore all of the charge will indeed be collected before the next pulse arrives.

The recombination proceeds only in the region of overlap of the positive and negative charge distributions following an instantaneous burst of radiation, and the *overlap time* is given by[2]

$$t_o = \frac{d^2}{(k_1 + k_2)V} = \frac{(0.615)^2}{(1070 + 1350)194} = 0.81 \ \mu\text{s},$$

which is much larger than the duration of the pulse itself. Accordingly, Boag's theory for

Class II recombination is applicable and the *collection efficiency*, f, can be obtained using

$$f = \frac{1}{u} \ln(1+u),$$

where

$$u = \frac{\mu d^2}{V} \rho_0,$$

and where $\mu = 1090$ V-cm/esu is an experimentally determined constant for air [2]. The average current, corrected for recombination, is then simply obtained from $I = fI_0$. Corrections are made in the following section ranging from $f = 0.91$ to $f = 0.47$ for values of I_{beam} varying from 0.5 to 3.5×10^{10} e^-/p, respectively.

6. Comparison of Measured and Calculated Results

In Figures 2a-c we compare EGS4-simulated IC currents with the experimental results from Table 1 (DC shifts subtracted). As stated earlier the saturation current, I_0, is clearly not attained over the entire range of beam currents for any of the three stopper configurations. However, when corrected for recombination, there is fairly good agreement for the two cases where the beam always strikes ST-1 (Figures 2a and 2b). This agreement becomes even more appreciated if one takes into account the relatively large (and systematic) spread of the experimental points themselves, which we suggest might be explained by inaccurate lateral positioning of the two chambers, or by asymmetric beam delivery (or both).

In the case of Figure 2c (ST-2 Only), the calculated curve for $Z = 60$ cm is systematically greater than the experimental data. However, as suggested by the energy-deposition histogram for 'ST-2 Only' (see Figure 1), a very small shift in the Z-position of the chambers can result in a significant change in F, and therefore I. This is demonstrated in Figure 2c where the dashed line corresponds to a calculation that uses the value of F at $Z = 52$ cm, which is a shift in position that is less than the diameter of the IC itself. Also, as expected, the 8-cm Z-shift is not as important for the ST-1 Only and ST-1 plus ST-2 cases.

Since the ion chambers were positioned along the beamline by eye, this could explain the differences that we have observed. For the most part, however, the agreement between calculation and measurement is rather encouraging.

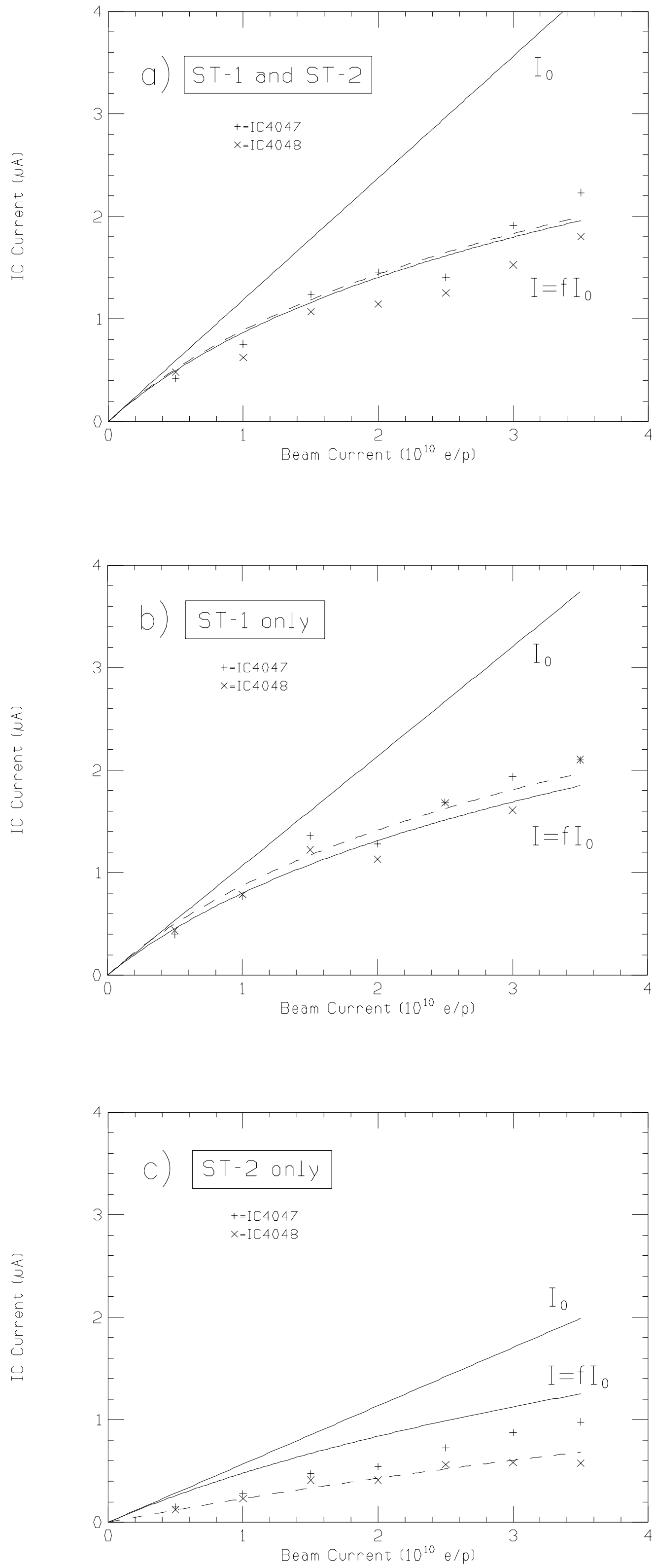

Fig 2. Average currents for three stopper configurations. Experiment: + and x. Calculation: solid line ($Z = 60$ cm) and dashed line ($Z = 52$ cm).

7. LOCATING IC-PAIRS BASED ON I VS. F

When deciding where the best location would be for placing a single IC-pair in a two-stopper system, the question naturally arises as to whether it is really necessary to plot the (corrected) average current as a function of Z, or whether the F histograms themselves will suffice. In Figure 3 we have plotted I as a function of Z for I_{beam} values of 0.5 and 3.5×10^{10} e^{-}/p. In both cases the crossover points are at $Z = 72$ cm, which also agrees with the crossover point for F in Figure 1. We conclude that we can simply use the energy-deposition histograms.

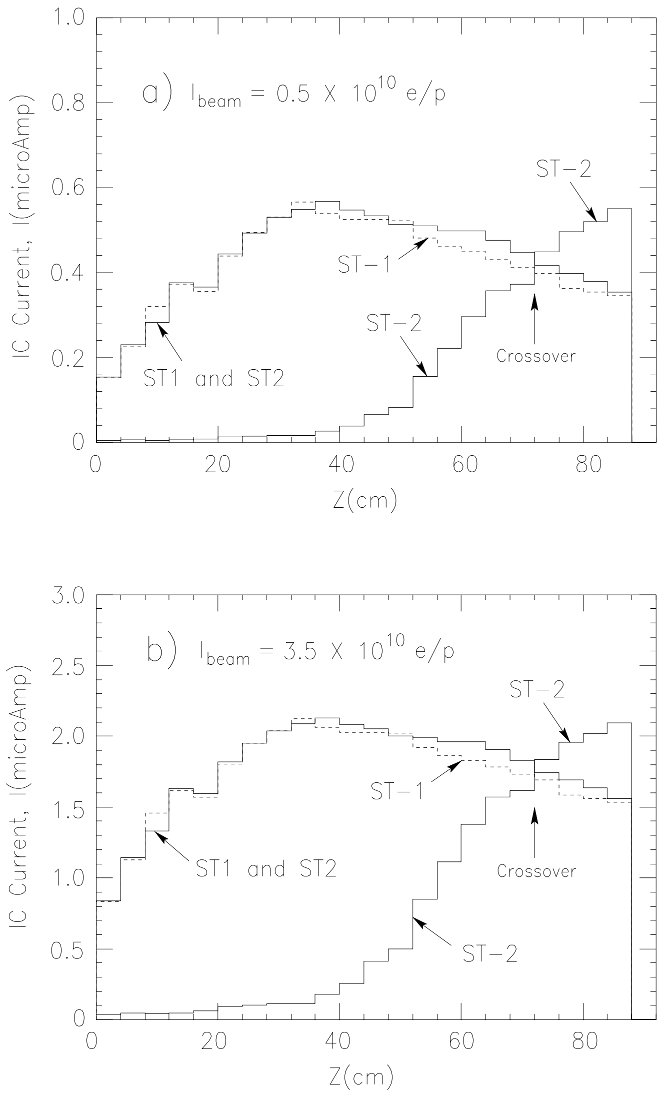

Fig 3. Average current vs. Z. a) $I_{beam} = 0.5 \times 10^{10}$ e^{-}/p, b) $I_{beam} = 3.5 \times 10^{10}$ e^{-}/p.

8. Concluding Remarks

We have demonstrated experimentally that we can use the EGS4 code to calculate the average current that is measured by an air-filled ion chamber placed near stoppers that are struck by high-energy electron beams, provided that pulsed-beam recombination is properly taken into account.

Because the ionization rate in the experiment that we have presented were rather high, correction factors in the range of $0.5 < f < 0.9$ were necessary. The pulsed-beam recombination theory of Boag[2], on the other hand, is generally only applicable when $f > 0.7$. Nevertheless, we used it since it was the only easy-to-use theory available, and with apparent success.

We have also demonstrated that we actually do not have to calculate the (corrected) average current, I, in order to decide where to place the IC-pair along the beamline, but we can simply rely on the crossover point of the energy-deposition histograms themselves.

REFERENCES

1. W. R. Nelson, H. Hirayama, and D. W. O. Rogers, "The EGS4 Code System", SLAC-265 (1985).
2. J. W. Boag, "Ionization Chambers". In Radiation Dosimetry, Vol. II (F. H. Attix and W. C. Roesch, eds.), Chapter 9, Academic Press, Second Edition (1966).